

Calcium phosphate coatings: Morphology, micro-structure and mechanical properties

Saeed Saber-Samandari^{a,*}, Kadhim Alamara^b, Samaneh Saber-Samandari^c

^aNew Technologies Research Centre, Amirkabir University of Technology, Tehran, P.O. Box 1591633311, Iran

^bIRIS, Faculty of Engineering and Industrial Sciences, Swinburne University of Technology, Hawthorn, VIC 3122, Australia

^cDepartment of Chemistry, Eastern Mediterranean University, Gazimagusa, TRNC via Mersin 10, Turkey

Received 10 May 2013; accepted 9 June 2013

Available online 19 June 2013

Abstract

Many biomedical implant coating systems consist of micro-deposited calcium phosphate droplets thermally sprayed onto a commercially pure Ti (CP Ti) substrate. In this study, the morphology of solidified droplet “splats” was examined using Scanning Electron Microscopy (SEM). The topography of splats sprayed onto substrates at room temperature (25 °C) and preheated to 100 °C and 300 °C was investigated. The splat shape was found to be strongly dependent on substrate preheating temperature. A homogeneous deposit density of amorphous calcium phosphate in splats deposited onto the cold substrate was confirmed by micro-Raman spectroscopy, whereas a very early stage of re-crystallization was detected using Transmission Electron Microscopy (TEM) for splats deposited onto 300 °C preheated substrates.

TEM in conjunction with Focused Ion Beam (FIB) revealed the splats' ultra micro-structure. Correlation of Atomic Force Microscopy (AFM) with these results enabled links between different types of micro-structures and true splat contacts with the substrates to be shown. Splats deposited onto the substrate at 300 °C showed generally well-adherent interfaces. The established presence of a thin layer of native oxide on this polished and preheated surface could serve to enhance the splat-substrate adhesion.

Nano-indentation revealed that splats deposited onto the substrates at room temperature and 100 °C have similar hardness and elastic modulus values; however, preheating the substrate up to 300 °C improved these micro-mechanical properties.

These combined findings promote further understanding of the extrinsic properties of the bulk calcium phosphate coating.

© 2013 Elsevier Ltd and Techna Group S.r.l. All rights reserved.

Keywords: C. Mechanical properties; Calcium phosphate; Morphology; Microstructure

1. Introduction

Thermal spray coatings are formed from individual molten particles that spread and solidify to create single solidified droplets as they impact on a substrate. The flattened and hardened particles take various shapes and are called “splats”. They represent the building blocks of a whole coating. Coating characteristics are dictated by the manufacturing process, but enhanced understanding of the desirable characteristics requires consideration of the geometrical form, micro-structure and micro-mechanical properties. It is the first layer of splats

which determines the coating-substrate adhesion, while the coating cohesion is determined by the nature of the inter-splat contact. Although research has been directed towards bulk coatings, a recent emphasis has examined individual splats as a means to obtaining a deeper understanding of coating properties [1–4].

Splat morphology has an important effect on coating quality and is a function of process parameters such as particle size, impact velocity [5], and substrate condition [6]. It is also related to the substrate temperature [7,8]. Preheating the substrate prior to thermal spraying can prevent splashing and also reduce the gas that may become trapped between the splat and the substrate. The first analytical model of particle flattening was developed in 1983 [9] and succeeding work has been either experimental [10] or numerical modeling [11]

*Corresponding author. Tel.: +98 21 6696 4418.

E-mail addresses: saeedss@aut.ac.ir,
sabersamandari@yahoo.com (S. Saber-Samandari).

in nature. Most studies on the effect of substrate temperature on the morphology of single splats have investigated High Velocity Oxy-Fuel (HVOF) or plasma spraying [12,13]. Little work has been done on splats generated by other thermal spray processes such as flame spraying, in which powders are injected into a flame torch of lower temperature and velocity than that of the HVOF and plasma spraying methods.

The first part of the current study examines the effect of substrate preheating on splat morphology of calcium phosphate coatings produced by the flame spraying method. Hydroxyapatite ($\text{Ca}_{10}(\text{PO}_4)_6(\text{OH})_2$) is a biocompatible material resembling the mineral component of bone and teeth, and finds application in forming functional coatings on biomedical implant devices. In this study, hydroxyapatite powder particles are deposited onto commercially pure titanium (CP Ti) substrates at room temperature, 100 °C and 300 °C. The aim is to establish the minimum temperature where a disk splat is formed without any splashing, i.e., the “transition temperature”, as first defined by Fukumoto et al. [14]. Disk splats produce nearly fully dense coating, while splashed splats produce highly porous coating and are desirable for cell proliferation [15].

Research on the micro-structure of single splats of molten calcium phosphate is limited. The coating obtained mainly comprises hydroxyapatite, but other crystalline and amorphous calcium phosphate phases are also present. The micro-structure of thermally-sprayed hydroxyapatite splats and the formation mechanism of micro-pores within the splats has been investigated using TEM [16]. In the present study, attention is given to the effect of preheating the substrate with regard to the splat micro-structure.

The primary interest of many studies, however, has been the bonding of the coatings to substrates, which is determined by the strength of the bond between the first splat and the coated surface. As a fundamental approach to determining coating reliability, the third aim of this study is to consider the bonding between individual splats and the substrates. Exposing the interface using a conventional cross-section preparation technique is a complicated task. The FIB apparatus offers the possibility of preparing such cross-sections. Only a few reports on FIB-assisted cross-sectioning of a splat are available to date [17–19].

Measurements of mechanical properties such as hardness and elastic modulus have been performed to understand and improve the coating quality for long-term stability of an implant material. This study examines the micro-mechanical properties of splats using nano-indentation techniques. Nano-indentation methods have been successfully developed for testing single solidified micro-sized deposits [3,4,20].

2. Experimental procedures

2.1. Substrate preparation

The commercially pure titanium (CP Ti) substrates were surface finished by grinding with a semi-automatic polisher using SiC papers (800, 1200 and 2500 grit), followed by

mirror polishing on a Dur surface instrument (Struers, Denmark) with 3 μm and 1 μm diamond suspensions. The flat surface was cleaned in an ultrasonic bath with isopropyl alcohol to remove any remaining residue.

2.2. Feedstock powders and coating production

Hydroxyapatite powder (CAM implants, Netherlands) was sieved to a particle size of $30 \pm 10 \mu\text{m}$. Characterization has been documented in a different paper that has used the same powder [21]. This powder was delivered from the powder feeder (Metco 3MP, Sulzer Metco, Wohlen, Switzerland) into a flame spray torch (Metco 5P, Sulzer Metco, Wohlen, Switzerland) operated with acetylene and oxygen, with air as a carrier gas at a rate of 3 g/min. This relatively low powder feed rate allowed the particle flux to be controlled so that the likelihood of producing individual, non-overlapping particles was enhanced. A typical production feed rate of 25 g/min would produce similar particle morphologies; however, individual characteristics would be confounded due to mutual interactions. The polished substrates were positioned 13 cm from the torch and the powder sprayed onto the CP Ti, with the surface at room temperature or preheated to 100 °C and 300 °C before coatings, to produce flattened solidified droplets with a round shape and minimal splashes. Details of reference samples (i.e. amorphous calcium phosphate and sintered hydroxyapatite) have been documented in an early study [4].

2.3. Micro-Raman spectroscopy

Micro-Raman provides a capability to identify the bonding within calcium phosphates and distinguish between different crystalline phases. This is crucial with thermally sprayed hydroxyapatite powders that can undergo phase decomposition or form an amorphous phase under rapid cooling conditions. The micro-deposit was located with a $100\times$ objective in the optical microscope and analysis was conducted using a Raman Renishaw RM1000 micro-spectrometer (Renishaw, UK) with an excitation wavelength of 514 nm and a spectral resolution of 1 cm^{-1} . Spectra were recorded within the range of 800–1100 cm^{-1} to show the most intense peak for calcium phosphates.

2.4. Scanning Electron Microscopy (SEM) and Atomic Force Microscopy (AFM)

The calcium phosphate splat surface was observed using a conventional SEM (ZEISS SUPRA 40VP). The sample was gold coated using a DYNAVAC CS300 coating unit before being mounted on pin-type aluminum SEM mounts with double-sided conducting carbon tape. AFM (MFP-3D, Asylum Research) was performed to determine the topography of deposited droplets.

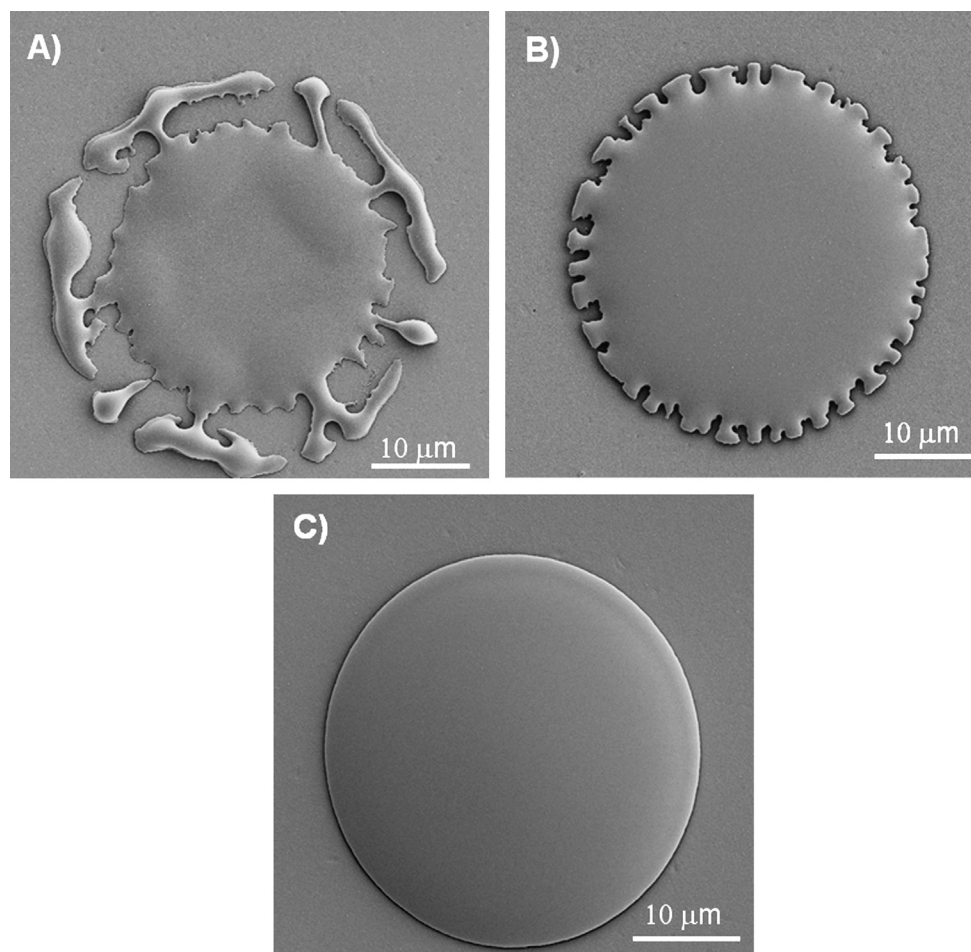


Fig. 1. Typical topographical morphology of flame sprayed calcium phosphate splats deposited onto the CP Ti substrates (A) at room temperature, (B) preheated to 100 °C and (C) preheated to 300 °C.

2.5. Transmission Electron Microscopy (TEM) and Focused Ion Beam (FIB)

TEM imaging was carried out using an FEI Tecnai TF20 field emission gun transmission electron microscope operating at 200 kV. TEM sample preparation was performed with a Nova Nanolab dual-beam FIB system using a 30 keV gallium beam. Prior to FIB examination, the TEM specimen area of interest was coated with a 1 μm thick platinum protective film using the electron beam deposition facility of the FIB system. Cross-sectional TEM samples were prepared using the *in situ* lift out method.

2.6. Nano-indentation

Depth-sensing indentation measured the mechanical properties. The NanoTest (MicroMaterials, UK) is a pendulum-based depth-sensing system that applies a force electromagnetically to conduct a nano-indentation experiment. The elastic modulus and hardness were calculated from the load-depth penetration curve of a Berkovich indenter (a three-sided pyramid with a total included angle of 142.3°), based on the methods proposed by Oliver and Pharr [22]. All indentations were made on the

top of splats and in a well-defined flat region to avoid either overestimation or underestimation of the indent area [23]. The diamond area function was calibrated by indenting into a reference sample (i.e. fused silica) to determine the true contact area for a given depth. This experimental procedure is necessary due to rounding of the indenter tip.

3. Results and discussion

3.1. Morphology of the calcium phosphate coating

The substrate temperature plays an important role in splat formation. The typical morphology of calcium phosphate splats deposited onto substrates at different temperatures is illustrated in Fig. 1. The results clearly reveal the differences in splat morphology that arise from differing substrate temperatures. The frequency of occurrence of disk splats was determined for three different substrates at each temperature. Irregular-shaped splats were obtained from thermal spraying onto the room temperature surface (Fig. 1A). The degree of splashing can be minimized by heating up the substrate. A splat deposited onto the substrate preheated to 100 °C displays a disk shape with some irregularity at the rim

Table 1
Transition temperature for different powder materials.

Materials	Spraying device	Coating	Substrate	Transition temp.	Author
Metal	Plasma spray	Zirconia	Stainless steel	250–300 °C	Sampath et al. [7]
Metal	Wire arc spray	Aluminum	AISI 304L	230 °C	Abedini et al. [41]
Metal	Plasma spray	Copper	AISI 304	300 °C	Yang et al. [42]
Glass	Plasma spray	Soda lime silicate	AISI 316L	170 °C	Poirier et al. [43]
Ceramic	Plasma spray	Alumina	AISI 304	318 °C	Tanaka et al. [44]
Ceramic	Plasma spray	Titanium dioxide	AISI 304	350 °C	Tanaka et al. [44]
Ceramic	Plasma spray	Yttria-stabilized zirconia	AISI 304	340 °C	Tanaka et al. [44]
Polymer	Flame spray	Polypropylene	Microscope glass	25 °C	Alamara et al. [45]

(Fig. 1B) while a perfect regular disk shape is observed from preheating the substrate to 300 °C, Fig. 1C. The implication is that there is a transition temperature for each coating material that demarks a shape transition from a splashed form to a regular disk (see Table 1). For calcium phosphate, the transition temperature was determined to be 300 °C. This transition temperature appears to be independent of the splat melting point (around 1550 °C). An increase in the temperature of the substrate leads to a decrease in the contact thermal resistance (due to decomposition of impurities at the interface) and to an increase in the heat removal from the splat [24]. Therefore, splashes vanish, providing a perfect disk-shaped splat. Splashing occurs on a cold substrate surface due to lack of desorption of adsorbates, poor wettability and rapid solidification [25]. A coating which contains splashed splats at coating-substrate interface promotes the formation of pores and poor adhesion.

3.2. Characterization of the calcium phosphate coating

The highly disordered materials (i.e. those that are so irregular that the concept of a reference crystal lattice must be abandoned) are called amorphous materials [26]. Raman micro-probe spectroscopy produces a $\nu_1\text{PO}_4$ band broad peak at 950 cm^{-1} for amorphous calcium phosphate and a sharp peak at 960 cm^{-1} for sintered hydroxyapatite (see Fig. 2). The broad peak thus serves as an identifier for amorphous calcium phosphate. A broad peak at $\sim 950\text{ cm}^{-1}$ was also observed for the splats deposited onto the 25 °C, 100 °C and 300 °C CP Ti substrates. Formation of the amorphous phase could have arisen from the high gun traverse speed over the substrate allowing rapid cooling, and supported by dehydroxylation. If a cooling rate is faster than the rate at which atoms can be organized into a more thermodynamically favorable crystalline state, then an amorphous solid will be formed. The Raman peak intensity is lower for splats compared to the annealed amorphous reference sample. This characteristic has been used to distinguish amorphous calcium phosphate; however, bands at the same position as those of amorphous calcium phosphate might also be due to disordered domains arising, for example, from the drying of surface hydrated layers of poorly crystalline apatite [27]. Other investigations providing evidence for the presence of distinct amorphous and crystalline phases are therefore required. Further, the splat deposited onto the 300 °C preheated substrate reveals a brighter central area on

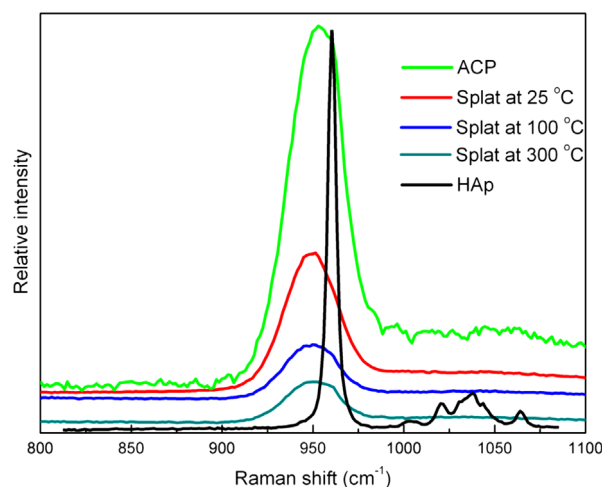


Fig. 2. Representative Raman spectra of five of the types of samples studied: amorphous calcium phosphate, splats deposited onto CP Ti at 25, 100 and 300 °C, and sintered hydroxyapatite. Splats have the same signature as amorphous calcium phosphate.

the splat (see SEM images in Fig. 8). The top of the splat will be the last to solidify and therefore have the highest probability of crystallization. A powerful tool to study such fine microstructures could be TEM.

Results of TEM studies of thermal sprayed calcium phosphates are very scarce. The main reason is the difficulty in preparing the very brittle thin electron-transparent specimens required. Fig. 3A shows the amorphous calcium phosphate phase observed under TEM in individual splats deposited onto a room temperature substrate. The same selected area electron diffraction (SAED) patterns show diffused rings for splats deposited onto the preheated substrate at 100 °C. This is a characteristic of the amorphous structure. Formation of this amorphous phase is attributed to the rapid quenching associated with thermal spraying, whereas preheating the substrate to 300 °C is likely to have partially cleaned the surface of adsorbates thus improving the heat transfer rate between the splat and the substrate. The SAED pattern in Fig. 3B contains dots along with diffused rings. The co-existence of dots and diffused rings in the SAED patterns of calcium phosphate splats indicates the simultaneous presence of amorphous and crystalline phases, Fig. 3B. No such dotted SAED pattern is found in splats deposited onto the substrates held at 25 °C or

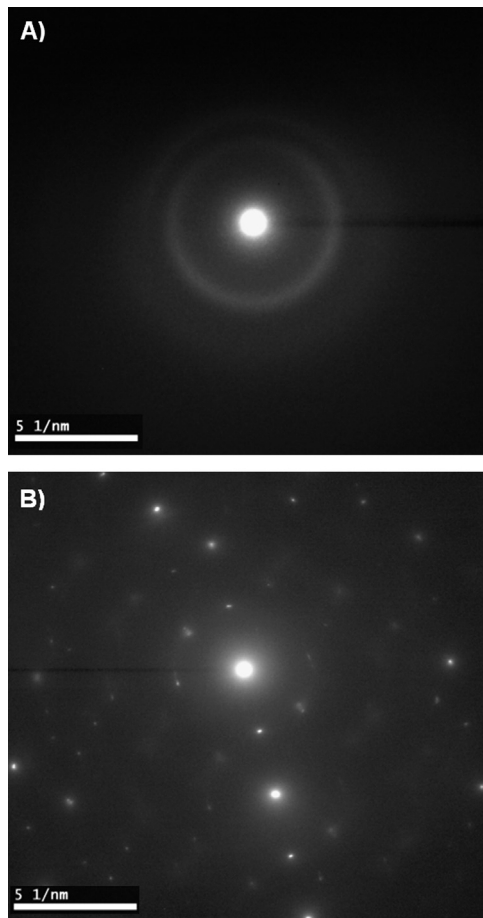


Fig. 3. Diffraction patterns (TEM) from individual calcium phosphate splats deposited onto the CP Ti substrate, showing (A) a typical amorphous structure for a splat deposited onto the room temperature substrate and (B) re-crystallization stage for a splat deposited onto the substrate preheated to 300 °C. Examination of several other splats deposited onto the substrate preheated to 300 °C indicated that there is neither amorphous structure nor preferred crystal orientation but rather a very early stage of re-crystallization.

100 °C. These results lead to the conclusion that the set of splats deposited onto the preheated substrate at 300 °C are at an early stage of re-crystallization (crystalline islands form along with the amorphous phases); while the other two sets of splats are likely to contain a large amount of amorphous phase.

The choice of calcium phosphate coatings depends on the site and extent of the bone defect. Amorphous calcium phosphate should be present in only moderate quantities because of its fast dissolution, which promotes fast fixation to bone tissue [27]. A minimal amount of amorphous calcium phosphate is also needed to ensure good adhesion of the coating to the metallic prosthesis [28,29]. Crystallized hydroxyapatite is more stable and better suited to slow remodeling.

3.3. Adhesion of the calcium phosphate coating

3.3.1. Single layer

The coating must be sufficiently well adhered to the underlying substrate to provide any practical benefit. Upon impact, an

impinging molten droplet has the highest kinetic and thermal energies. During spreading, the liquid flows radially outwards, expanding the splat area and increasing the contact between splat and substrate. Preheating the substrate aids in wider interfacial contact beneath the splat and allows development of stronger adhesions through bonding mechanisms like chemical reactions.

The TEM represents a suitable tool for characterization of the splat-substrate adhesion properties. Fig. 4A–C shows step-by-step the complex specimen preparation stages for FIB. Fig. 4D clearly reveals delamination at the edge of the splat deposited onto the cold substrate. Neither signs of delamination in the splat rim nor pores/ micro-cracks in the splat middle were detected for more than ten splats deposited onto the 300 °C preheated substrate, Fig. 4E. This suggests that these splats possess high adhesion strength and can be explained by the evaporation and desorption of air molecules that occurs at a hot surface. This mechanism acts to clean the surface of any impediments to droplet spreading. It can be noted that adsorption of moisture on the surface of the substrate is expected under ambient conditions.

Another hypothesis for the cause of the delamination seen in Fig. 4D is the existence of residual stresses. Two stresses occur in a thermal spraying process: quenching stress (developed in the splat immediately after impact) and cooling stress (which develops as the splat cools down to room temperature together with the substrate). Quenching stress is originally tensile, while cooling stress depends on the coefficients of thermal expansion of the coating and substrate. In the case of calcium phosphate deposited onto CP Ti, the direction of cooling stresses is also tensile [21]. Therefore, one would expect tensile residual stresses in calcium phosphate deposited onto CP Ti. As a consequence of the release of these residual stresses, either a micro-crack or delamination along the interface is expected. Evidence of this delamination has been shown using FIB on a splat cross-section, Fig. 4D. In order to confirm this hypothesis, besides some current attempts on residual stress measurements [30], strong efforts are still needed to develop new cutting edge methodologies for measuring stresses in poorly crystalline or amorphous materials with sub-micrometer resolution.

At the splat-substrate interface, a ~20 nm thick titanium oxide layer with nano-scale roughness was found extending uniformly over the length of the splat cross-section, Fig. 5. This ceramic layer was created during the preheating of the substrate to 300 °C carried out in ambient conditions. The thickness of this layer and alternatively its roughness increase as the substrate temperature is increased. For instance, the oxide thickness on stainless steel 316L is 25 nm at 250 °C, 40 nm at 400 °C and 58 nm at 580 °C [31]. Adhesion of the TiO₂ ceramic layer, grown during the atmospheric preheat, to the CP Ti metal substrate is assumed to be excellent. The overall adhesion of splats to the polished preheated substrate is provided almost exclusively by chemical bonding and is qualitatively very high [32]. In fact, adhesion measurements of coatings sprayed on polished, preheated and oxidized substrates showed an increase in adhesion strength by a factor of two in comparison with standard coatings sprayed on room temperature substrates [33].

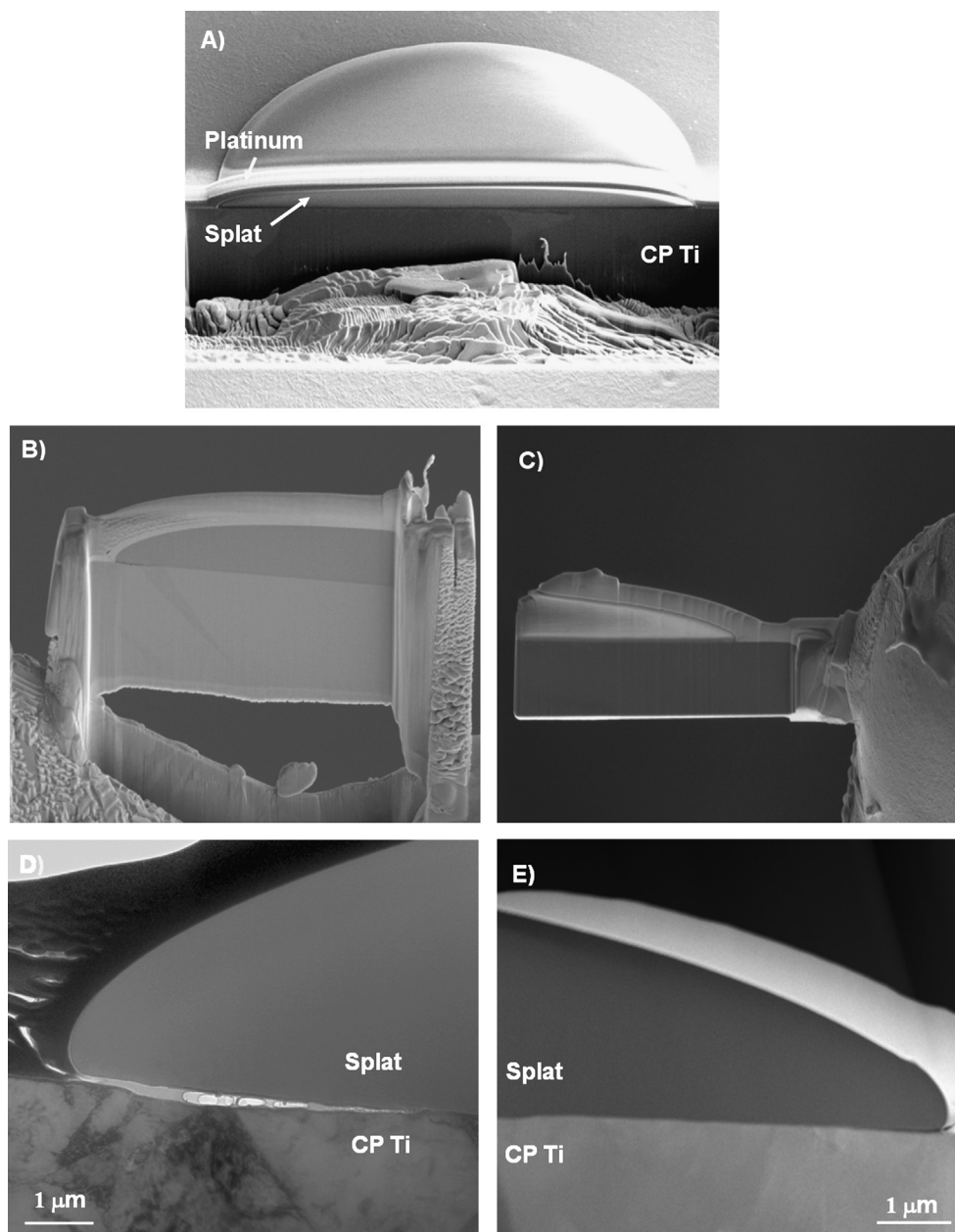


Fig. 4. For preparation of a TEM sample, a FIB instrument is used to produce a thin lamella. (A) An FIB image of a single solidified calcium phosphate droplet deposited onto CP Ti substrate. The bright areas over the selected area are platinum layers deposited to protect the area of interest from beam damage. (B) Milling of the lamella and making it ready for lifting out of the substrate. (C) Attaching the lamella to a TEM grid for further thinning. (D) Delamination at the edge of the splat deposited onto CP Ti at room temperature. (E) A well-bound splat deposited onto the 300 °C preheated substrate.

3.3.2. Multi layer

Though the spraying technique used in this study was tailored to produce single calcium phosphate splats on the CP Ti substrate, it also occasionally yielded multi-layer (i.e. double and triple) splats, Fig. 6. When two or more droplets happen to impinge on the substrate at the same location within a very short period of time, a splat–splat interface is formed. All subsequent splats examined adhered well to the initial splat and no delamination was observed by SEM, Fig. 6. A few micro-cracks were noted on the surface of splats deposited onto the room temperature substrate, Fig. 6A. The continuity of the cracks across the splat surface indicates that these cracks formed due to the contraction of the upper splat during

cooling. Surprisingly, no such micro-cracks were found on the splat surface (even in the third layer) deposited onto the 300 °C preheated substrate, Fig. 6B. From the morphology point of view, for the upper-deposited splats, the ‘substrate’ becomes considerably rougher. Therefore, the spreading and solidification processes will no longer produce regular circular splats of uniform thickness, Fig. 6. Solidification shrinkage and cooling contraction will give rise to residual stresses, since the splats will not be free to accommodate the shape of the roughness. In terms of micro-structure, however, there is a hypothesis that the first layer of splats, which is directly deposited onto the metallic surface, undergoes a faster cooling and develops an amorphous phase. The subsequent splats cool

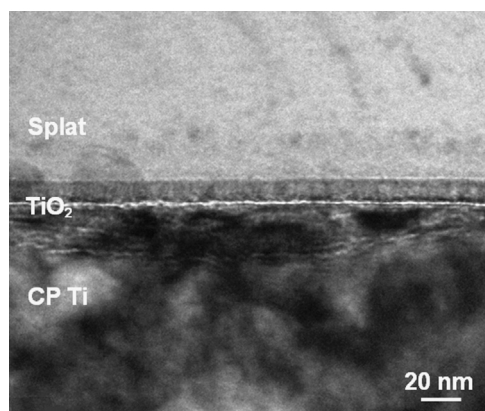


Fig. 5. An FIB image of the interface between a single solidified calcium phosphate droplet and a 300 °C preheated CP Ti substrate showing the thin layer of ceramic TiO₂.

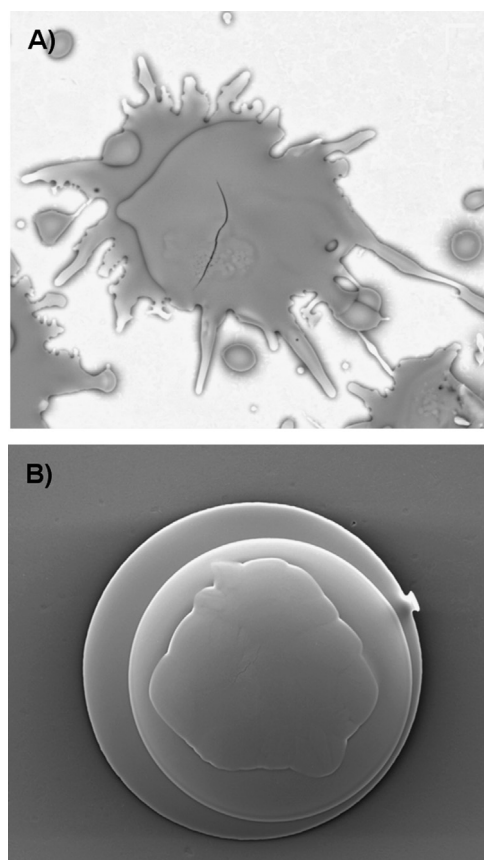


Fig. 6. Multiple calcium phosphate splats deposited onto CP Ti: (A) room temperature substrate, (B) 300 °C preheated substrate.

at a lower rate because they are deposited onto a pre-existing ceramic layer with lower thermal conductivity than the metallic substrate, and so can develop some crystalline phases [18]. In a previous study this hypothesis has been confirmed for a complete flame-sprayed coating of calcium phosphate [34].

3.4. Mechanical properties of the calcium phosphate coating

Nano-indentation experiments were performed on the top of splats in locations that were well-defined as being flat regions

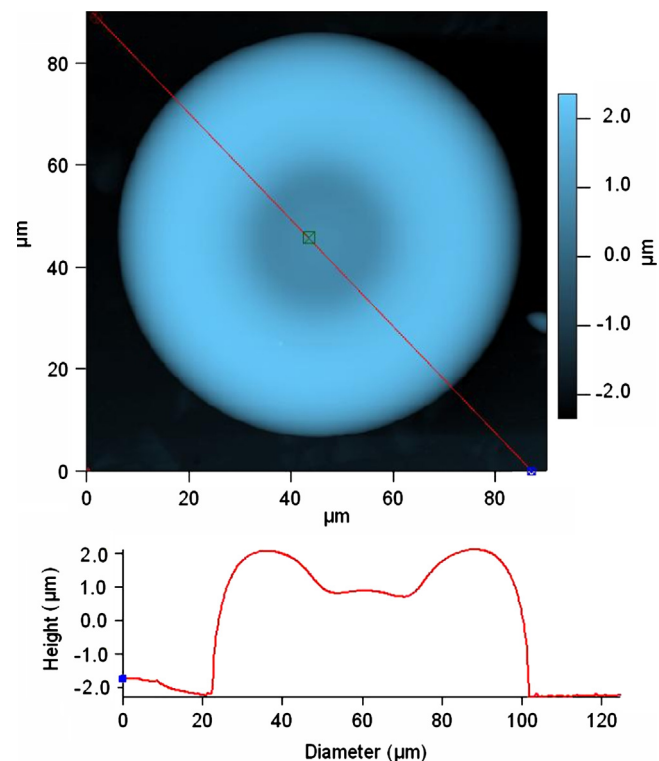


Fig. 7. Topographic image of single solidified calcium phosphate splat taken by non-contact mode scanning (set amplitude=5 nm). Also shown below the image is the height profile along a line marked in the image.

to avoid either overestimation or underestimation of the indent area [23]. The diamond area function was calibrated by indenting into a fused silica reference sample to determine the true contact area for a given depth. A commonly used rule is that the penetration depth should not exceed 10% of the coating thickness [35]; however, it has been found that this rule is too restrictive for soft films and may not be sufficiently restrictive for hard films. In the case of a soft film on a hard substrate a relative indentation depth of 50% confers negligible deviations from the true film hardness [36]. For a hard film on a soft substrate, an indentation depth of 7–15% of the film thickness yields accurate values [37,38]. This relationship, though, depends on the combinations of the film-substrate systems and is more sensitive to differences in the elastic properties than in the plastic properties of the coating-substrate system [39].

In this study, the results are averaged over 8 indentations to a depth of 200 nm and represent 7–8% of the film thickness (height measurements on a few splats revealed a splat thickness of $\sim 3 \mu\text{m}$ in the central region [21], Fig. 7). A Poisson's ratio of 0.28 was assumed in calculating the elastic moduli of splats [40]. Splats deposited onto the 300 °C preheated CP Ti substrate exhibited a modulus of $99 \pm 3 \text{ GPa}$, while those deposited at 25 °C and 100 °C showed a lower modulus, Table 2. Splats deposited onto the preheated substrate at 300 °C also demonstrate the highest hardness value of $4.4 \pm 0.1 \text{ GPa}$ compared to the others with $3.9 \pm 0.3 \text{ GPa}$.

The differences in mechanical properties are deemed to arise from the substrate preheating, since all other conditions were not altered. Preheating a substrate can change the residual stresses

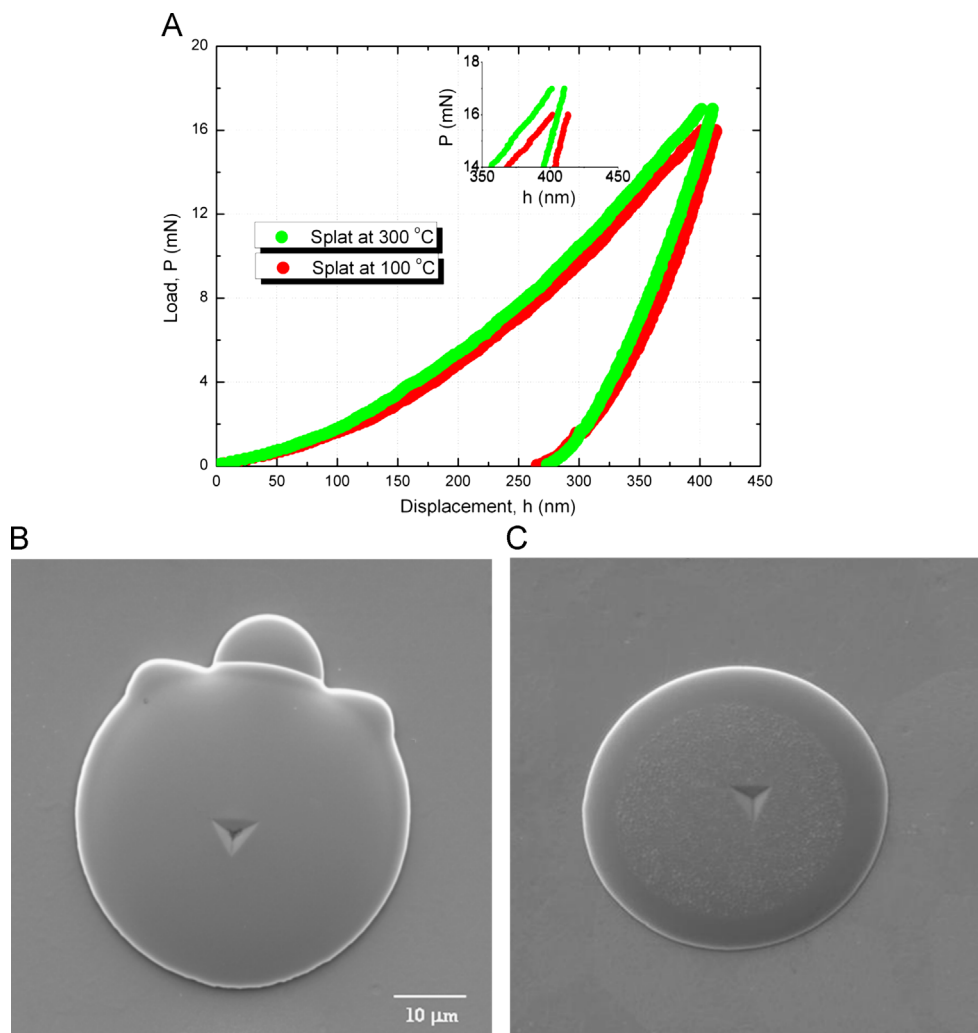


Fig. 8. (A) Load–displacement responses obtained upon indenting calcium phosphate splats deposited onto substrates at 100 °C and 300 °C using a Berkovich indenter, showing the indentation depth and final displacement of 400 nm and ~260 nm, respectively. Before the real test, the area function for the diamond was calibrated by indentation in fused silica to determine the contact area for a given depth. Contact area as a function of depth was found $A(h_c) = 22h_c^2 + 2500h_c$ by the polynomial-fitting procedure. The measured depth was then adjusted for the effect of instrument compliance (0.499 nm/mN) in the instrument software for analysis. The hardness and reduced modulus of fused silica, assuming a Poisson's ratio of 0.165, were measured to be 8.8 ± 0.1 and 69.6 ± 0.2 GPa, respectively. (B) SEM image of a single solidified calcium phosphate droplet deposited onto the 100 °C preheated CP Ti substrate showing a residual indentation at the center. (C) SEM image of a single solidified calcium phosphate droplet deposited onto the 300 °C preheated CP Ti substrate showing a residual indentation at the center.

Table 2
Micro-mechanical properties of calcium phosphates.

Mechanical property	Splat at 25 °C	Splat at 100 °C	Splat at 300 °C	Amorphous coating [46]	Crystalline coating [47]	Sintered hydroxyapatite [4]	Single crystal [48]
H (GPa)	3.9 ± 0.3	3.9 ± 0.2	4.4 ± 0.1	1.5 ± 0.3	5.4 ± 0.5	6.9 ± 0.4	7.1 ± 0.3
E (GPa)	91 ± 4	91 ± 3	99 ± 3	48 ± 6	118 ± 7	127 ± 2	150 ± 2

within the splat, as well as its micro-structure. The elastic modulus is an intrinsic property of the material and should not be influenced by residual stresses. The variation in mechanical properties is also present throughout the splat, as confirmed by nano-indentation to a greater depth of 400 nm, Fig. 8A. Loads of 17.2 mN and 15.9 mN were required to reach the same penetration depth for splats deposited onto the substrates preheated to

300 °C and 100 °C, respectively. Fig. 8B and C illustrates splats deposited onto the CP Ti substrates preheated to 300 °C and 100 °C, respectively, where residual indentations after the completion of the experiments are observed in the center region.

Substrate heating transforms the micro-structure, as can be observed in splats that exhibit two different porosities, Fig. 9A and B. The porosity seen for the splat deposited onto the 300 °C

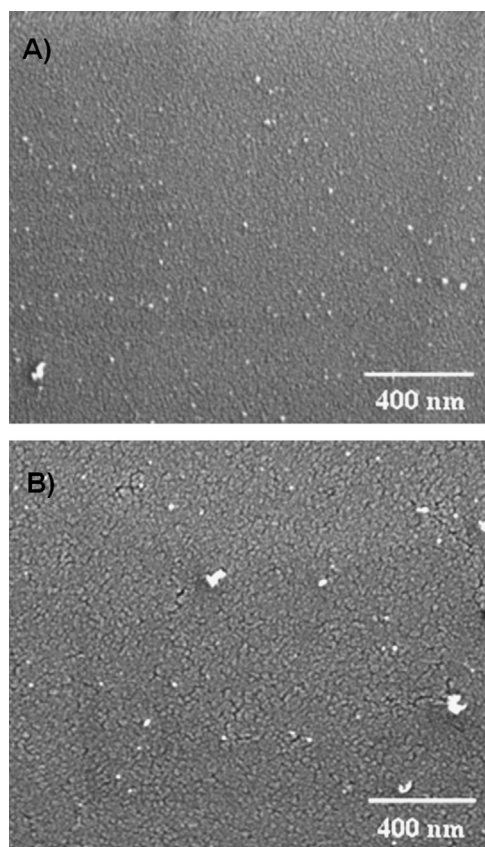


Fig. 9. SEM images from the center region of calcium phosphate splats deposited onto the substrates preheated to (A) 100 °C and (B) 300 °C, showing the fine microstructure.

preheated substrate suggests that the middle of the splat is the last portion to solidify, and solidification seems to begin from the rim of the splat. The solidification rate is higher on a cold substrate, which favours the formation of denser splats (Fig. 9A), compared to those deposited onto a hot substrate (Fig. 9B). At high solidification rates, for example, when the splat is deposited onto a room temperature substrate, trapped gases are retained and sealed micro-pores may be created within the coating rather than at its surface. An important implication of this finding is that nano-indentation methods, which are themselves ascribed to intrinsic properties, can now also be considered as extrinsic in nature since the ultra micro-structure is examined. Within a well-defined fabrication and testing protocol where similar micro-structures are observed, then the case for splats representing the intrinsic building blocks of coatings is more valid.

Although some work on single splats has been reported recently, very little information is available on the ‘second’ splat. Investigation of the micro-structure and micro-mechanical properties of this second splat could provide a fundamental approach to determining coating reliability. Further work in this direction is being carried out by the author.

4. Conclusions

The effect of substrate temperature on the morphology of calcium phosphate splats deposited onto CP Ti was studied.

A transition temperature exists above which a regular disk shape splat can be formed; preheating the substrate increases the wetting and the effective contact area for the splat, leading to formation of a disk shape. Less than 5% of splats formed disk splats at 25 °C, increasing to more than 50% and 95% at 100 °C and 300 °C, respectively.

The amorphous calcium phosphate phase was observed with micro-Raman spectroscopy, while an early re-crystallization stage was confirmed using TEM for splats deposited onto the substrates preheated to 300 °C.

The FIB-assisted SEM imaging is an excellent tool for studying the splat-substrate interface. Spraying of amorphous calcium phosphate onto a substrate preheated to 300 °C, rather than a cold substrate, can lead to improved adhesion between the coating and substrate. Good interfacial contact was observed between amorphous calcium phosphate and the preheated CP Ti. Preheating improves the spreading of the splat by allowing more time for cooling and removing volatile adsorbates on substrates. It was found that the oxide ceramic layer (TiO₂) on the surface of the 300 °C preheated substrate remained intact across the entire splat–substrate interface. The presence of this ceramic layer could promote establishment of chemical bonds between the splat and the substrate.

Splats deposited onto a substrate preheated to 300 °C exhibit higher modulus and hardness values compared with those deposited onto cold substrates.

Acknowledgments

The authors thank Prof. Christopher C. Berndt of Swinburne University of Technology and Dr. Karlis A. Gross of Riga University for their support and encouragement of this research. The authors thank Dr. Paul Spizzirri of The University of Melbourne for his help with the Micro-Raman spectroscopy and Dr. Sergey Rubanov of Bio 21 institute for their generous help in providing the TEM and FIB images. Dr. Ray Dagastine of The University of Melbourne is acknowledged for his advice and assistance regarding AFM.

References

- [1] M. Psandideh-Fard, V. Persin, S. Chandra, J. Mostaghimi, Splat shapes in a thermal spray coating process: simulations and experiments, *Journal of Thermal Spray Technology* 11 (2002) 206–217.
- [2] H. Li, B.S. Ng, K.A. Khor, P. Cheang, T.W. Clyne, Raman spectroscopy determination of phases within thermal sprayed hydroxyapatite splats and subsequent in vitro dissolution, *Acta Materialia* 52 (2004) 445–453.
- [3] S. Saber-Samandari, K.A. Gross, Amorphous calcium phosphate offers improved crack resistance—a design feature from nature, *Acta Biomaterialia* 7 (2011) 4235–4241.
- [4] S. Saber-Samandari, K.A. Gross, The use of thermal printing to control the properties of calcium phosphate deposits, *Biomaterials* 31 (2010) 6386–6393.
- [5] M. Vardelle, A. Vardelle, A.C. Leger, P. Fauchais, D. Gobin, Influence of particle parameters at impact on splat formation and solidification in plasma spraying processes, *Journal of Thermal Spray Technology* 4 (1995) 50–58.
- [6] H. Li, S. Costil, H.L. Liao, C.J. Li, M. Planche, C. Coddet, Effects of surface conditions on the flattening behavior of plasma sprayed Cu splats, *Surface and Coatings Technology* 200 (2006) 5435–5446.

- [7] S. Sampath, X.Y. Jiang, J. Matejcek, A.C. Leger, A. Vardelle, Substrate temperature effects on splat formation, microstructure development and properties of plasma sprayed coatings Part I: case study for partially stabilized zirconia, *Materials Science and Engineering: A* 272 (1999) 181–188.
- [8] M. Fukumoto, E. Nishioka, T. Matsubara, Flattening and solidification behaviour of a metal droplet on a flat substrate surface held at various temperatures, *Surface and Coatings Technology* 120–121 (1999) 131–137.
- [9] J. Madejski, Droplets on impact with a solid surface, *Int. Journal of Heat and Mass Transfer* 26 (1983) 1095–1098.
- [10] G. Montavon, S. Sampath, C.C. Berndt, H. Herman, C. Coddet, Effects of vacuum plasma spray processing parameters on splat morphology, *Journal of Thermal Spray Technology* 4 (1995) 67–74.
- [11] J.P. Delplanque, R.H. Rangel, An improved model for droplet solidification on a flat surface, *Journal of Materials Science* 32 (1997) 1519–1530.
- [12] J. Mostaghimi, M. Passandideh-Fard, S. Chandra, Dynamics of splat formation in plasma spray coating process, *Plasma Chemistry and Plasma Processing* 22 (2002) 59–84.
- [13] S. Sampath, X. Jiang, Splat formation and microstructure development during plasma spraying: deposition temperature effects, *Materials Science and Engineering: A* 304–306 (2001) 144–150.
- [14] M. Fukumoto, S. Katoh, I. Okane, Splat behavior of plasma sprayed particles on flat substrate surface, in: A. Ohmori (Ed.), *Thermal Spraying—Current Status and Future Trends*, High Temperature Society of Japan, Osaka, Japan, 1995, pp. 353–359.
- [15] Y. Huang, L. Song, X. Liu, Y. Xiao, Y. Wu, J. Chen, F. Wu, Z. Gu, Hydroxyapatite coatings deposited by liquid precursor plasma spraying: controlled dense and porous microstructures and osteoblastic cell responses, *Biofab* 2 (2010) 045003.
- [16] H. Li, K.A. Khor, P. Cheang, Thermal sprayed hydroxyapatite splats: nanostructures, pore formation mechanisms and TEM characterization, *Biomaterials* 25 (2004) 3463–3471.
- [17] H.R. Salimi-Jazi, L. Pershin, T.W. Coyle, J. Mostaghimi, S. Chandra, Y.C. Lau, L. Rosenzweig, E. Moran, Effect of droplet characteristics and substrate surface topography on the final morphology of plasma-sprayed zirconia single splats, *Journal of Thermal Spray Technology* 16 (2007) 291–299.
- [18] L. Li, B. Kharas, H. Zhang, S. Sampath, Suppression of crystallization during high velocity impact quenching of alumina droplets: observations and characterization, *Materials Science and Engineering: A* 456 (2007) 35–42.
- [19] S. Brossard, P.R. Munroe, A.T.T. Tran, M.M. Hyland, Study of the effects of surface chemistry on splat formation for plasma sprayed NiCr onto stainless steel substrates, *Surface and Coatings Technology* 204 (2010) 1599–1607.
- [20] K.A. Gross, S. Saber-Samandari, Nano-mechanical properties of hydroxyapatite coatings with a focus on the single solidified droplet, *Journal of the Australian Ceramic Society* 43 (2007) 98–101.
- [21] S. Saber-Samandari, C.C. Berndt, K.A. Gross, Selection of the implant and coating materials for optimized performance by means of nanoindentation, *Acta Biomaterialia* 7 (2011) 874–881.
- [22] W.C. Oliver, G.M. Pharr, Measurement of hardness and elastic modulus by instrumented indentation: advances in understanding and refinements to methodology, *Journal of Materials Research* 19 (2004) 3–20.
- [23] S. Saber-Samandari, K.A. Gross, Effect of angled indentation on mechanical properties, *Journal of the European Ceramic Society* 29 (2009) 2461–2467.
- [24] V.V. Sobolev, Formation of splat morphology during thermal spraying, *Materials Letters* 36 (1998) 123–127.
- [25] M. Fukumoto, T. Yamaguchi, M. Yamada, T. Yasui, Splash splat to disk splat transition behavior in plasma-sprayed metallic materials, *Journal of Thermal Spray Technology* 16 (2007) 905–912.
- [26] Y.T. Cheng, W.L. Johnson, Disordered materials: a survey of amorphous solids, *Science* 235 (1987) 997–1002.
- [27] C. Combes, C. Rey, Amorphous calcium phosphates: synthesis, properties and uses in biomaterials, *Acta Biomaterialia* 6 (2010) 3362–3378.
- [28] Y.C. Tsui, C. Doyle, T.W. Clyne, Plasma sprayed hydroxyapatite coatings on titanium substrates. Part 2: optimisation of coating properties, *Biomaterials* 19 (1998) 2031–2043.
- [29] R.B. Heimann, R. Wirth, Formation and transformation of amorphous calcium phosphates on titanium alloy surfaces during atmospheric plasma spraying and their subsequent in vitro performance, *Biomaterials* 27 (2006) 823–831.
- [30] M. Sebastiani, G. Bolleli, L. Lusvardi, P.P. Bandopadhyay, E. Bemporad, High resolution residual stress measurement on amorphous and crystalline plasma-sprayed single-splats, *Surface and Coatings Technology* 206 (2012) 4872–4880.
- [31] S. Chandra, P. Fauchais, Formation of solid splats during thermal spray deposition, *Journal of Thermal Spray Technology* 18 (2009) 148–180.
- [32] T. Chruska, A.H. King, Transmission electron microscopy study of rapid solidification of plasma sprayed zirconia—Part II. Interfaces and subsequent splat, *Thin Solid Films* 397 (2001) 40–48.
- [33] H.-D. Steffens, B. Wielage, J. Drozak, Interface phenomena and bonding mechanism of thermally-sprayed metal and ceramic composites, *Surface and Coatings Technology* 45 (1991) 299–308.
- [34] S. Saber-Samandari, K.A. Gross, Nanoindentation reveals mechanical properties within thermally sprayed hydroxyapatite coatings, *Surface and Coatings Technology* 203 (2009) 1660–1664.
- [35] W.C. Oliver, G.M. Pharr, An improved technique for determining hardness and elastic modulus using load and displacement sensing indentation experiments, *Journal of Materials Research* 7 (1992) 1564–1583.
- [36] X. Chen, J.J. Vlassak, Numerical study on the measurement of thin film mechanical properties by means of nanoindentation, *Journal of Materials Research* 16 (2001) 2974–2982.
- [37] M. Lichinchi, C. Lenardi, J. Haupt, R. Vitali, Simulation of Berkovich nanoindentation experiments on thin films using finite element method, *Thin Solid Films* 312 (1998) 240–248.
- [38] X. Cai, H. Bangert, Hardness measurements of thin films—determining the critical ratio of depth to thickness using FEM, *Thin Solid Films* 264 (1995) 59–71.
- [39] Z.-H. Xu, D. Rowcliffe, Finite element analysis of substrate effects on indentation behaviour of thin films, *Thin Solid Films* 447–448 (2004) 399–405.
- [40] G. DeWith, H.J.A. VanDijk, N. Hattu, K. Prijs, Preparation, microstructure and mechanical properties of dense polycrystalline hydroxyapatite, *Journal of Materials Science* 16 (1981) 1592–1598.
- [41] A. Abedini, A. Pourmousa, S. Chandra, J. Mostaghimi, Effect of substrate temperature on the properties of coatings and splats deposited by wire arc spraying, *Surface and Coatings Technology* 201 (2006) 3350–3358.
- [42] K. Yang, M. Fukumoto, T. Yasui, M. Yamada, Study of substrate preheating on flattening behavior of thermal-sprayed copper particles, *Journal of Thermal Spray Technology* 19 (2010) 1195–1205.
- [43] T. Poirier, P. Planche, O. Landemarre, C. Coddet, Particles spreading phenomena in the case of glass thermal spraying, *Journal of Thermal Spray Technology* 17 (2008) 564–573.
- [44] Y. Tanaka, M. Fukumoto, Investigation of dominating factors on flattening behavior of plasma sprayed ceramic particles, *Surface and Coatings Technology* 120–121 (1999) 124–130.
- [45] K. Alamara, S. Saber-Samandari, C.C. Berndt, Splat formation of polypropylene flame sprayed onto a flat surface, *Surface and Coatings Technology* 205 (2010) 2518–2524.
- [46] K.A. Gross, S. Saber-Samandari, K. Heeman, Evaluation of commercial implants with nanoindentation defines future development needs for hydroxyapatite coatings, *Journal of Biomedical Materials Research Part B* 93 (2010) 1–8.
- [47] S. Saber-Samandari, K.A. Gross, Nanoindentation on the surface of thermally sprayed coatings, *Surface and Coatings Technology* 203 (2009) 3516–3520.
- [48] S. Saber-Samandari, K.A. Gross, Micromechanical properties of single crystal hydroxyapatite by nanoindentation, *Acta Biomaterialia* 5 (2009) 2206–2212.